3rd National Congress on Physical Sciences, 29 Sep. – 2 Oct. 2016, Sofia
Section: Physics of Earth, Atmosphere and Space

Tsunami Radiation Pattern from Seismic Sources in the Black Sea

Lyuba Dimova[*1], **Alberto Armigliato**[2], **Gianluca Pagnoni**[2], **Stefano Tinti**[2], **Reneta Raykova**[1]

[1]Department of Meteorology and Geophysics, Faculty of Physics, St. Kliment Ohridski University of Sofia, 5 James Bourchier Blvd., BG-1164 Sofia, Bulgaria
[2]Department of Physics and Astronomy, Sector of Geophysics, University of Bologna, Bologna, Italy

Abstract. This study is focused on the tsunami radiation pattern from the most important seismic sources in the Black Sea. The tsunami impact on the coastal area of the Black Sea is discussed by comparing historical data and numerical results. Several potentially tsunamigenic earthquake sources are identified in this study and different simulations are performed, by means of the numerical code UBO-TSUFD. We consider earthquakes with magnitude M_W between 5.5 for the shelf zone near Ukraine and 8.0 for the south-eastern part of the Black Sea. Different characteristic and parameters of the seismic sources are proposed. To see local effects of tsunami radiation pattern, in the calculation we use 30s-resolution bathymetry data. Results are given through the distribution of the maximum positive and negative tsunami sea surface elevations induced by the generated tsunamis.

1 Introduction

Tsunamis are gravity waves that propagate across the ocean. They are caused by earthquakes, landslides, caldera collapses, volcanic eruptions or any impacts that perturb the ocean water masses. Tsunamis occur most frequently in the Pacific, generated by strong earthquakes from so called “Pacific Ring of Fire”, but they occur also in the European waters due to earthquakes caused by the African Plate drifting northwards underneath the Eurasian Plate. Ten percent of all tsunamis worldwide occur in the Mediterranean region and adjacent seas. In this study, we are focused in modeling earthquake-induced tsunamis in the Black Sea. The examination of the sources of generated in the past tsunamis is a difficult task because some of them are caused by earthquakes followed by landslides, and some of them have an unclear origin. Totally 23 historical tsunamis were identified since first century B.C. [1–6] that are reported

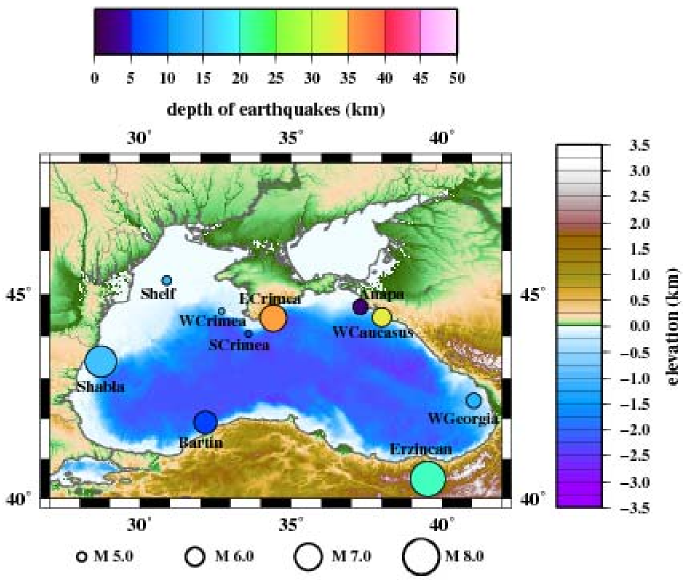

Figure 1: Earthquake epicenters with color depth scale and circle diameter scaled to magnitude.

to have occurred in the Black Sea. We identified the tsunamigenic areas where the earthquake epicenters are focused (Figure 1). Most of the events occurred near the Bulgarian, the Ukrainian and the Turkish Black Sea coasts. Few, but destructive events happened near the coastline of Georgia and Russia.

Table 1: List of fault parameters (Bulgarian, Ukrainian seismic zones)

zone/ parameters	Shabla NE-SW	Shabla W-E	Balchik	Shelf	Western Crimea	Southern Crimea	Eastern Crimea
L (km)	64	64	64	4.4	8.5	8.5	32
W (km)	29	29	29	3.2	5.5	5.5	17
D (m)	3.5	3.5	3.5	0.5	0.8	0.8	2.0
$Strike$ (°)	30	305	280	122	130	240	50
Dip (°)	80	82	82	86	70	80	50
$Rake$ (°)	150	26	26	270	90	90	270
$Depth$ (m)	2000	2000	2000	1000	1000	2000	2000
M_W	7.5	7.5	7.5	5.5	6.0	6.0	7.0

Table 2: List of fault parameters (Russian, Georgian, Turkish seismic zones).

zone/ parameters	Western Caucasus	Western Georgia	NW Turkey	NE Turkey
L (km)	8.5	16.6	32	125
W (km)	5.5	9.5	17	50
D (m)	0.8	1.2	2.0	6.0
$Strike$ (°)	105	20	238	108
Dip (°)	60	60	62	86
$Rake$ (°)	270	150	76	90
$Depth$ (m)	2000	3000	3000	4000
M_W	6.0	6.5	7.0	8.0

We named the studied tsunamigenic areas according to the geographical location. They are as follow: for the Bulgarian Black Sea coast we consider Shabla NE-SW, Shabla W-E and Balchik fault zones; for the Ukrainian coastline — Shelf, Western Crimea, Southern Crimea and Eastern Crimea fault zones; for the Turkish and east shore of Black Sea — NW Turkey and NE Turkey, Western Caucasus and Western Georgia, respectively.

2 Theory and Methodology

2.1 Computing the initial conditions of tsunami source

The problem of computing the displacement fields associated to point-source dislocation or to a rectangular fault source in a homogeneous half-space bounded by a free surface was studied and solved by Steketee [7, 8] and Okada [9, 10]. The analytical solutions by Okada were employed to obtain the displacements due to an elastic dislocation at the free surface. We estimated the coseismic deformation as a function of the fault geometry and the elastic parameters of the medium. We calculated the seismic moment M_0 in N*m of a particular event by means of the simple relation (1), proposed by Hanks and Kanamori [11]:

$$\log(M_0) = 1.5 \times M_W + 16.1 \tag{1}$$

Mai and Beroza [12] suggested the following regressions to obtain the relations between the fault geometry and the seismic moment:

$$\log(L) = -5.20 + 0.35 \times \log(M_0) \tag{2}$$

$$\log(W) = -4.28 + 0.29 \times \log(M_0) \tag{3}$$

$$\log(D) = -4.98 + 0.35 \times \log(M_0) \tag{4}$$

where L is the length of fault in km, W is width of fault in km, and D is the displacement over the fault in m.

Focal mechanism solutions for the selected sources are taken from recent large earthquakes occurred in the area, assuming that they do not change over time for the same seismic zone. Data is provided by the International Seismological Centre Bulletin (`http://www.isc.ac.uk/iscbulletin/search/fmechanisms/`) and by the TRANSFER Project (`http://www.transferproject.eu/`). Geometry fault parameters of the hypothetical seismic sources are listed in Table 1 and Table 2. $Depth$ in the tables is referred to the depth of the fault's top.

2.2 Computing tsunami propagation

Numerical simulations are useful tools in tsunami research since they can be used to reconstruct recent and historical events or to create forecasts of tsunami impact and inundation in early warning systems [13]. Tsunami simulations in this study were performed by means of the numerical code UBO-TSUFD. The code has been developed at the University of Bologna, Italy and is based on the non-linear shallow water (NSW) theory in a Cartesian frame. The Coriolis terms are neglected since in the Black Sea all main tsunami effects occur within a time interval too short for the Coriolis condition to be effective. UBO-TSUFD uses a staggered grid and an explicit leapfrog finite-difference method. The bottom friction f is taken into account [14]. The horizontal components of the velocities are constant along the water column. NSW equations hold under the assumptions of pressure hydrostaticity and of fluid incompressibility, so the vertical component of fluid particles acceleration is negligible compared to the gravity acceleration. The NSW equations are presented as:

$$\frac{\partial M}{\partial t} + \frac{\partial}{\partial x}\left(\frac{M^2}{D}\right) + \frac{\partial}{\partial y}\left(\frac{MN}{D}\right) + gD\frac{\partial \eta}{\partial x} + f_x = 0 \tag{5}$$

$$\frac{\partial N}{\partial t} + \frac{\partial}{\partial x}\left(\frac{MN}{D}\right) + \frac{\partial}{\partial y}\left(\frac{N^2}{D}\right) + gD\frac{\partial \eta}{\partial y} + f_y = 0 \tag{6}$$

$$\frac{\partial \eta}{\partial t} + \frac{\partial M}{\partial x} + \frac{\partial N}{\partial y} = 0 \tag{7}$$

where η is the water surface elevation measured from the undisturbed sea surface, h is the undisturbed water depth, $D = h + \eta$ is the total water column, and the discharge fluxes M and N are related to the velocities u and v by the formulas:

$$M = u(h + \eta) = uD \tag{8}$$

$$N = \nu(h + \eta) = \nu D \tag{9}$$

The bottom friction components f_x and f_y are given in terms of the fluxes M, N, Manning's roughness coefficient n, and gravity constant g:

$$f_x = \frac{gn^2}{D^{7/3}} M \sqrt{(M^2 + N^2)} \quad (10)$$

$$f_y = \frac{gn^2}{D^{7/3}} N \sqrt{(M^2 + N^2)} \quad (11)$$

An option of the code UBO-TSUFD allows to be solved also a linear version of the NSW equations, where D is approximated by h and the advection terms in the momentum eqs. (6) and (7) are neglected.

3 Results

The results of the study present simple scenarios of earthquake-induced tsunamis in the Black Sea. Magnitudes M_W taken into account (given in Tables 1 and 2) are equal or larger than the highest magnitude registered in that study zone in historical times. Simulations give basic features of the tsunami propagation and point out the coastal areas where the

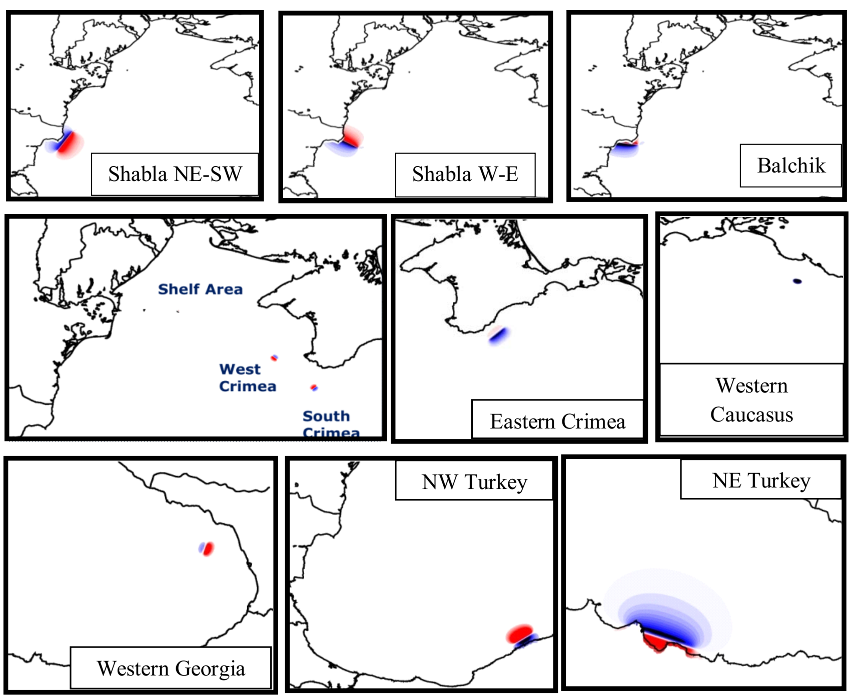

Figure 2: Initial tsunami conditions for each of the eleven hypothetical seismic sources considered in this study.

highest effects are expected. The initial tsunami conditions, computed on the basis of the fault parameters listed in Table 1 and Table 2, are plotted in Figure 2 for all scenarios.

3.1 Shabla NE-SW, Shabla W-E, Balchik

The history of earthquakes in the area of the Bulgarian Black Sea coast goes back to the first century B.C., when an earthquake caused landslides and a local tsunami. One of the well documented events with magnitude $M > 7.6$ took place in A.D. 543/544. According to Ranguelov et al. [15], the earthquake generated a tsunami that caused inundation in the city of Balchik. More recently, an earthquake-induced tsunami occurred in March 1901 ($M = 7.2$) [4]. We simulated three hypothetical sources. We utilized focal parameters from the earthquake of December 2012 for the Shabla NE-SW, focal parameters for Shabla W-E correspond to the event of August 2009, while we speculated for Balchik on the basis of the geotectonics of the area. The magnitude we chose is 7.5 in agreement with the length of the fault (around 64 km). The extreme initial sea elevation for these scenarios varies between -0.62 m (downlift) and 0.95 m (uplift). Simulations are performed for 5 hours travelling time, to observe the propagation of tsunami waves throughout the Black Sea (Figure 3). The effects of the simulated scenarios for Shabla NE-SW, Shabla W-E and Balchik are local with estimated negative and positive wave heights between -2.31 m and 3.22 m (Figure 4). All three sources are located close to the Bulgarian Black Sea coast and thus the lead time is less than 15 minutes.

3.2 Shelf

The shelf zone in the northwestern part of the Black Sea is characterized by earthquakes with magnitude lower than 5.5. An earthquake in January 1838 ($M = 7.3$) caused a tsunami destroying the harbor of Odessa, but it is considered indeed an event from the Vrancea seismic zone [16]. The angles determining the focal mechanism are taken from the more recent

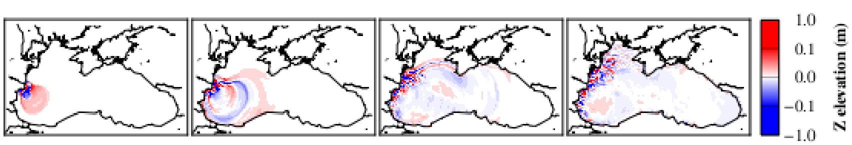

Figure 3: Tsunami scenario related to the hypothetical Shabla NE-SW earthquake source (snapshots of the computed water elevation fields are at 1000 s, 3000 s, 6000 s and 12000 s).

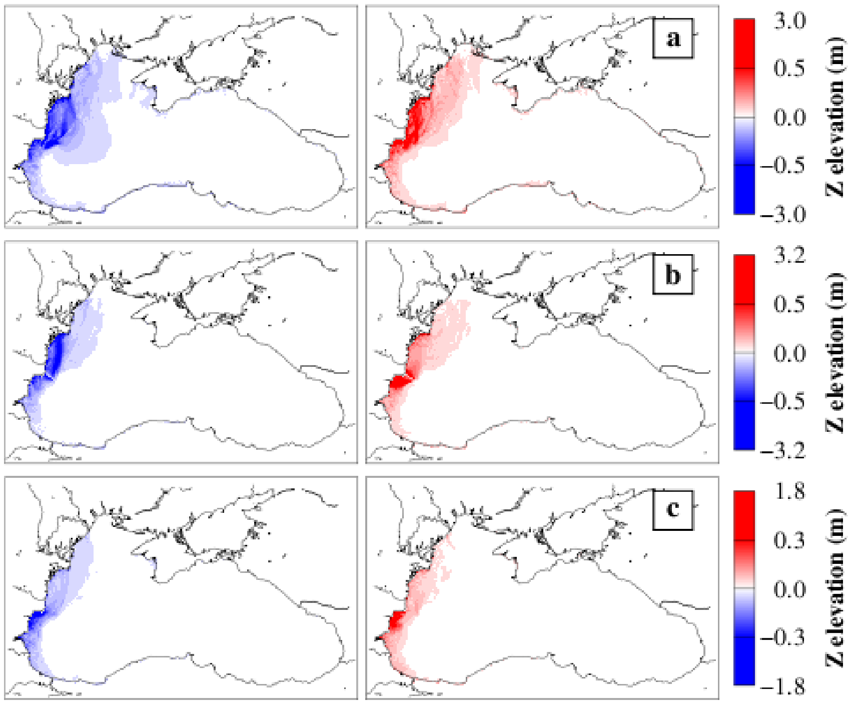

Figure 4: Extreme water elevation fields computed for the Shabla NE-SW (a), Shabla W-E (b) and Balchik (c) scenarios.

earthquake in March 1992. According to Okada's formulas, the computed vertical displacements for the initial conditions are -0.01 m (downlift) and 0.17 m (uplift). The maximum positive and negative computed water elevations are almost the same (Figure 5). The effects can be seen only near the source.

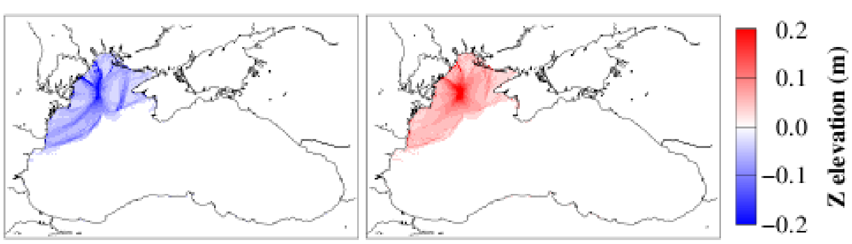

Figure 5: Extreme water elevation fields computed for the Shelf scenario.

3.3 Western Crimea, Southern Crimea and Eastern Crimea

There were several events in the past in the area of the Crimea peninsula. Numerical simulations were carried out for three hypothetical seismic sources, depicted in Figure 6. The western segment is located in the region of the last two (1945 and 1951) most powerful underwater earthquakes in the west part of the Black Sea ($M = 6.0$) [6]. The initial displacements of negative and positive heights are -0.13 m and 0.34 m respectively. The focal mechanism for this simulation was taken from an earthquake that occurred in August 1972. For the southern part of Crimea we considered a more recent event that took place in 1998, located near the slope of the peninsula. Historically, recorded magnitudes did not exceed 6. The tsunami effects of this hypothetical source are local. The initial deformations on the sea bottom are -0.19 m and 0.29 m, respectively for negative and positive elevations. Sea level disturbances during the simulation did not exceed ± 0.5 m. The eastern part corresponds to the region of seismic generation of the instrumen-

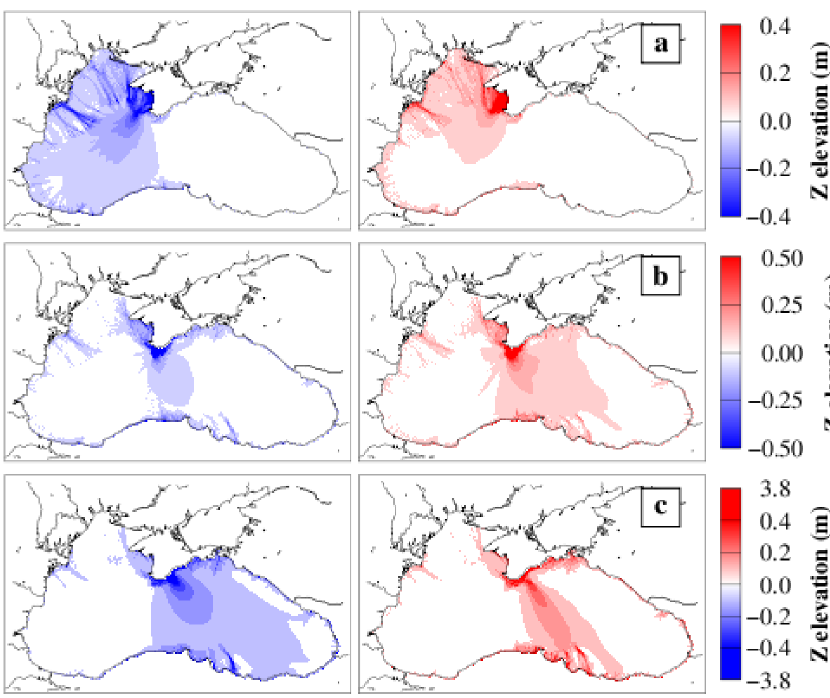

Figure 6: Extreme water elevation fields computed for the Western (a), Southern (b) and Eastern (c) Crimea scenarios.

tally recorded tsunami of September 12, 1927. The epicenter was located near the submarine slope, south of Yalta. Modeled extreme initial wave heights are -1.08 m and 0.16 m, while the maximum negative and positive simulated tsunami elevations are -3.24 m and 3.82 m. The energy of the tsunami propagates from north to south in less than one hour.

3.4 Western Caucasus

This region of Black Sea is associated with the Anapa earthquake that occurred on 12 July 1966 with magnitude of 5.8 and epicenter located approximately 10 km away from the shore [6]. The travel time of the tsunami to the Turkish coast is less than 40 minutes, while the Bulgarian coastline is reached within 1 hour and 20 minutes. The maximum and minimum initial water elevations are 0.03 m and -0.17 m respectively. The maximum positive sea elevations are not too high, compared to the amplitudes of the common storm waves [6]. The extreme tsunami wave heights computed for the Western Caucasus seismic source are plotted in Figure 7.

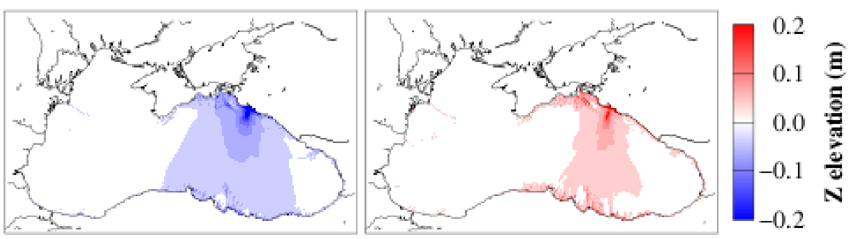

Figure 7: Extreme water elevation fields computed for the Western Caucasus scenario.

3.5 Western Georgia

The southeastern part of the Black Sea was hit by a tsunami triggered by a strong earthquake ($M > 6.5$) in the beginning of the first century A.D. We performed simulations by using the focal mechanism solution for the earthquake of December 2012. Maximum negative and positive vertical deformations of the tsunami initial condition are -0.09 m and 0.45 m respectively. The propagation of the waves is focused in the eastern part of the sea. The computed extreme tsunami heights are -0.78 m and 0.82 m, corresponding to negative and positive elevations (Figure 8).

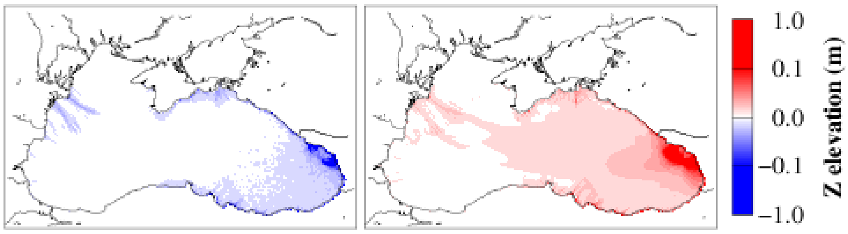

Figure 8: Extreme water elevation fields computed for the Western Georgia scenario.

3.6 NW Turkey and NE Turkey

Another tsunamigenic source close to the Black Sea is the North Anatolian Fault zone, capable of generating destructive earthquakes, like the August 1999 shock that triggered a tsunami in the Izmit Bay [1, 17]. A submarine earthquake caused significant damages in September 1968, where the coast of Amasra was flooded for about 100 m [5]. The focal mechanism of NW Turkey in this simulation is associated with this event. Figure 9 presents snapshots at 1000 s, 3000 s, 6000 s and 12000 s after the tsunami onset. The initial displacement field is characterized by a small downlift close to the coast and by uplift offshore [18]. The maximum uplift is 0.91 m, while the maximum downlift is -0.25 m. In the first quarter of an hour, the propagation of the tsunami basically reaches the northwestern part of Turkey. It is clear that after 50 minutes (3000 s) tsunami waves strike the Crimean peninsula. The tsunami covered the whole area of Black Sea in almost four hours.

The minimum and maximum tsunami elevations are displayed in Figure 10a. The fields can be interpreted as representation of the tsunami energy propagation. This "flow of energy" spreads along the western part of the Black Sea. There is almost no flux propagation towards the eastern part. The computed maximum and minimum heights are 3.54 m and -3.15 m respectively.

One of the key events ($M_S = 8.0$), near Erzincan, in 1939 that affected

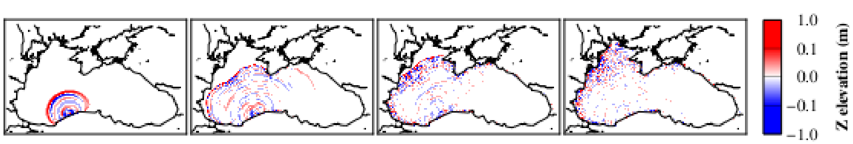

Figure 9: Tsunami scenario related to the hypothetical NW Turkey earthquake source.

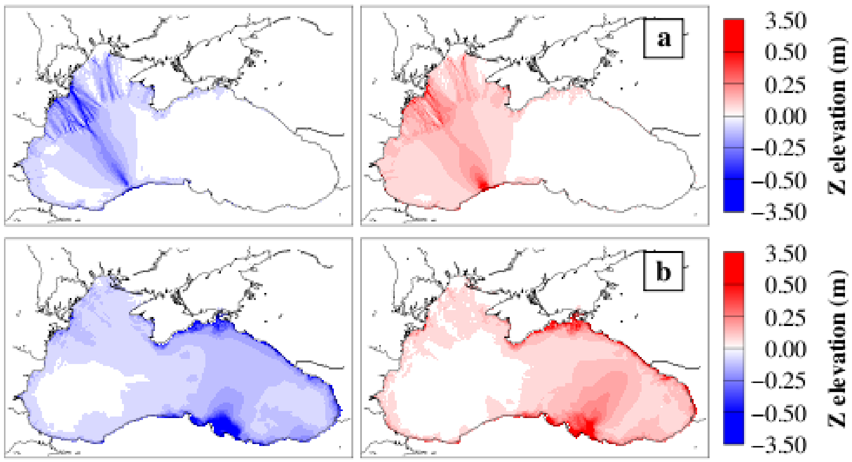

Figure 10: Extreme water elevation fields computed for the NW Turkey (a) and NE Turkey (b) scenarios.

several cities, is presented in Figure 10a. The earthquake epicenter was about 60 km inland. There is uncertainty on the real tsunami source: it could have been created directly by the main rupture or by a secondary fault or even by a submarine landslide in Black Sea, triggered by the earthquake [19]. We performed a scenario based on a secondary fault near the coastline offshore. The estimated heights of the tsunami waves vary from over 0.5 m for the Bulgarian, Ukrainian and Georgian coasts, up to 3 m for the western Caucasus and Turkish Black Sea coasts. In less than one hour waves hit the Ukrainian, Georgian and Russian coasts.

4 Conclusion

We compared historical data and geological maps for the area of Black Sea, to obtain the most relevant position of every seismic source discussed in the study. Several potentially tsunamigenic zones in the Black Sea are defined. We estimated the sea bottom deformation due to hypothetical seismic sources based on the Okada's analytical formulas. Numerical simulations for the propagation of the tsunami waves are performed using the code UBO-TSUFD. Maximum and minimum tsunami elevation fields are obtained. The selected focal mechanisms are in agreement with the geotectonics of the region and can be considered as typical for the generation of tsunami. The major effects considered for the Bulgarian Black Sea coast are associated with hypothetical seismic sources Shabla NE-SW and Shabla W-E. Simulations correspond to the historical information in the region. The eastern part of the Crimea peninsula is in the most threatened areas and suffers from local inundations induced by earthquakes located near the coast. Both of the considered faults near the Turkish Black Sea coast show great danger of flooding, not only locally but regionally because the associated magnitudes in that region are among the highest in the whole Black Sea. The tsunamis discussed in this paper should be investigated in more detail. Notice further that tsunamis near the steep slopes along the coast of Turkey can be triggered by earthquakes followed by landslides. Thus the effects would be larger. It would be of great interest to investigate tsunami caused by a probable subaerial landslide in the area of Cape Kaliakra.

Acknowledgement

The presented study is supported by project 215/2016 “Modeling of anomalous waves in the Black Sea” funded by Sofia University and Bulgarian Ministry of Education and Science.

References

[1] A. Maramai B. Brizuela and L. Graziani (2014) *Annals of Geophysics* **57** 4 S0435.

[2] G. A. Papadopoulos E. Gr?cia R. Urgeles V. Sallares P. M. De Martini D. Pantosti M. Gonzalez A. Yalciner J. Mascle D. Sakellariou A. Salamon S. Tinti V. Karastathis A. Fokaefs A. Camerlenghi T. Novikova and A. Papageorgiou (2014) *Marine Geology* **354** 81.

[3] G. A. Papadopoulos and A. Fokaefs (2005) *ISET J. of Earthquake Technology* **463** 42 4.

[4] B. Ranguelov S. Tinti G. Pagnoni R. Tonini F. Zaniboni and A. Armigliato (2008) *Geophysical Research Letters* **35** L18613.

[5] Y. Altinok and S. Ersoy (2000) *Natural Hazards* **21** 185.

[6] A. Yalciner E. Pelinovsky T. Talipova A. Kurkin A. Kozelkov and A. Zaitsev (2004) *Journal of Geophysical Research* **109** C12023.

[7] J. A. Steketee (1958a) *Can. J. Phys* **36** 192.

[8] J. A. Steketee (1958b) *Can. J. Phys* **36** 1168.

[9] Y. Okada (1985) *Bull. Seismol. Soc. Am.* **75** 1135.

[10] Y. Okada (1992) *Bull. Seismol Soc. Am.* **82** 1018.

[11] Th. C. Hanks and H. Kanamori (1979) *J. Geophys. Res.* **84** B5.

[12] P. M. Mai and G. C. Beroza (2000) *Bull. Seismol. Soc. Am.* **90** 3.

[13] S. Tinti and R. Tonini (2013) *Natural Hazards and Earth System Sciences* **13** 1759.

[14] R. Tonini A. Armigliato G. Pagnoni F. Zaniboni and S. Tinti (2011) *Nat. Haz. Earth Sys. Sci.* **11** 1217.

[15] B. Ranguelov E. Mircheva I. Lazarenko and R. Encheva (2008) In *Geoarchaeology and Archaeomineralogy: Proceed. of the Int. Conference, Sofia* **347**.

[16] G. A. Papadopoulos G. Diakogianni A. Fokaefs and B. Ranguelov (2011) *Nat. Haz. and Earth Sys. Sci.* **11** 945.
[17] Y. Altinok B. Alpar S. Ersoy and A. C. Yalciner (1999) *Turkish J. Marine Sciences* **5(3)** 131.
[18] S. Tinti A. Armigliato G. Pagnoni and F. Zaniboni (2005) *ISET J. of Earthquake Technology* **464** 42-4 171.
[19] U. Kuran and A. C. Yalciner (1993) In *Tsunamis in the World* **1** 159.